Journal of Sound and Vibration 333 (2014) 2040–2053

Contents lists available at ScienceDirect

Journal of Sound and Vibration

journal homepage: www.elsevier.com/locate/jsvi

Fokker–Planck equation analysis of randomly excited nonlinear energy harvester

P. Kumar [a], S. Narayanan [a], S. Adhikari [b,*], M.I. Friswell [b]

[a] Machine Design Section, Department of Mechanical Engineering, Indian Institute of Technology Madras, Chennai 600036, India
[b] College of Engineering, Swansea University, Singleton Park, Swansea SA2 8PP, UK

ARTICLE INFO

Article history:
Received 15 November 2012
Received in revised form
6 November 2013
Accepted 6 November 2013
Handling Editor: W. Lacarbonara
Available online 18 December 2013

ABSTRACT

The probability structure of the response and energy harvested from a nonlinear oscillator subjected to white noise excitation is investigated by solution of the corresponding Fokker–Planck (FP) equation. The nonlinear oscillator is the classical double well potential Duffing oscillator corresponding to the first mode vibration of a cantilever beam suspended between permanent magnets and with bonded piezoelectric patches for purposes of energy harvesting. The FP equation of the coupled electromechanical system of equations is derived. The finite element method is used to solve the FP equation giving the joint probability density functions of the response as well as the voltage generated from the piezoelectric patches. The FE method is also applied to the nonlinear inductive energy harvester of Daqaq and the results are compared. The mean square response and voltage are obtained for different white noise intensities. The effects of the system parameters on the mean square voltage are studied. It is observed that the energy harvested can be enhanced by suitable choice of the excitation intensity and the parameters. The results of the FP approach agree very well with Monte Carlo Simulation (MCS) results.

1. Introduction

Vibration based energy harvesting systems using piezoelectric, electromagnetic and electrostatic devices have been the subject of intense research in the last decade leading to efficient capturing of small amounts of energy from vibrating structures which when converted into electrical energy can be used to power micro and nano-electronic devices, sensors and recharge batteries. Significant research contribution in this area of vibration energy harvesting can be found in Refs. [1–7]. Several authors [8–10] considered the problem of determining optimal system parameters for maximizing the harvested energy.

Most of the early works in this area focused on systems subjected to deterministic excitation, typically to harmonic excitation. An important factor to be considered in these cases is to rely on the system performance near resonance requiring the frequency of excitation to be close to system natural frequency. Even slight deviation of the applied ambient excitation from the resonant condition resulted in significant reduction in the harvested energy. This led to the consideration of energy harvesters which are effective over a wide range of frequencies and to the study of their performance subjected to broad band random excitation. The consideration of random excitation has also to do with the fact that in many practical situations the ambient excitation could per se be stochastic. Lefeuvre et al. [10] were one of the first to

* Corresponding author. Tel: +44 1792 602088; fax: +44 1792 295676.
E-mail addresses: pankajiit1@yahoo.co.in (P. Kumar), narayans@iitm.ac.in (S. Narayanan), S.Adhikari@swansea.ac.uk (S. Adhikari), M.I.Friswell@swansea.ac.uk (M.I. Friswell).

0022-460X/$ - see front matter © 2013 Elsevier Ltd. All rights reserved.
http://dx.doi.org/10.1016/j.jsv.2013.11.011

investigate energy harvesting under random excitation. Soliman et al. [11] and Halvorsen [12] also investigated the performance of a vibration energy harvester under wide band random excitation. Adhikari et al. [13] using random vibration theory derived closed form expressions for the mean power harvested by a piezoelectric based energy harvester attached to a vibrating structure subjected to base Gaussian white noise random excitation. The systems considered in the above studies were linear systems.

It has been observed that nonlinear vibrating systems can be used as energy harvesters with bonded piezoelectric material for improved performance and effective operation over a range of frequencies. Erturk et al. [14], Stanton et al. [15] and Gammaitoni et al. [16] were a few of the researchers who investigated energy harvesting from nonlinear oscillators. They considered the excitation to be harmonic in their studies. Arrieta et al. [17] experimentally investigated energy harvesting from a bistable composite plate with bonded piezoelectric layers subjected to harmonic excitation. They exploited the rich nonlinear behaviour of the plate such as chaos and subharmonic motions and showed that sufficient energy can be extracted from the piezo-composite plate over a wide frequency range due to large amplitude vibrations. In these studies the excitation was assumed to be harmonic.

Recently, energy harvesting from nonlinear oscillators subjected to broad band random excitation has been the subject of investigation by a number of researchers. Litak et al. [18] investigated a nonlinear magneto piezoelectric energy harvesting system subjected to Gaussian band limited white noise excitation essentially by numerical simulation. The system considered by them was the classical double-well potential Duffing oscillator first studied by Moon and Holmes [19] to experimentally demonstrate chaos. The model considered by Litak et al. [18] consists of a cantilever beam suspended between permanent magnets at its free end to simulate the double well potential condition as in the Moon's experiment and subjected to base random excitation. The random excitation was assumed to be band limited Gaussian white noise. In the model, piezoelectric patches are bonded near the fixed end to make it as an energy harvester. Their study indicated that the nonlinear piezomagnetoelastic oscillator was most efficient as an energy harvesting device in specific ranges of the excitation intensity. Ali et al. [20] used the equivalent linearization method to analyze the above system and derived closed form approximate expressions for the response statistics and the mean square harvested energy. It was also shown by them that there exists an optimal value of the intensity of the excitation maximizing the mean harvested power.

The response of a dynamical system to white noise or delta correlated random excitation constitutes a Markov vector process whose transition joint probability density function (PDF) is governed by the Fokker–Planck (FP) equation. Exact solutions for the FP equation are available in the literature only for a few simple low dimensional nonlinear oscillators. In recent years, a number of efficient numerical methods for the solution of the FP equation of nonlinear systems subjected to random excitation have been developed such as the path integral (PI) method [21,22], the finite element (FE) method [23,24], and the finite difference method (FD) [24,25]. The advantage of the solution of the FP equation lies in the fact that the joint PDF of the response of the nonlinear system can be directly obtained. The response statistics and reliability estimates such as the first passage time and level crossing statistics can be obtained from the joint PDF.

In the context of the energy harvesting problem from randomly excited nonlinear systems, the solution of the corresponding Fokker–Planck–Kolmogorov (FPK) equation has been considered only by a few authors. Daqaq [26] obtained closed form solution of the FPK equation of an energy harvesting system of a bi-stable Duffing oscillator with double well potential connected to an inductive power generator. The inductive power generating mechanism results in a linear algebraic relation between the relative velocity of the nonlinear oscillator and the support and the voltage generated across the load resistance in terms of an electro-mechanical coupling coefficient. Using this relation in the oscillator equation of motion results in a second-order nonlinear system with an effective damping coefficient essentially retaining the original form of the Duffing oscillator. This enables obtaining a closed form solution of the corresponding stationary FPK equation as the product of two separable probability densities in terms of the displacement and velocity of the oscillator when the oscillator is subjected to support white noise excitation. The probability density function of the voltage will also be of the same form as the velocity as they are linearly related. They also considered the support excitation as belonging to the Ornstein–Uhlenbeck type with exponentially decaying auto-correlation function and obtained approximate solution of the FPK equation and the response statistics by an iterative process. This excitation was considered as the output of a first-order linear filter to white noise. They concluded that the expected value of the generated power is independent of the double well potential shape in the case of white noise excitation, while in the case the coloured noise excitation an optimum shape of the double well potential existed for maximum generated power.

In a recent paper, Green et al. [27] considered energy harvesting from a Duffing oscillator with viscous and coulomb damping subjected to support Gaussian white noise excitation. In this case, the oscillator is of the conventional single well potential of the hardening type and the energy harvesting mechanism is through an electro-magnetic device consisting of an electrical circuit with an inductive coil and resistance. The coil inductance and resistance as well as the load resistance were taken into account in the consideration of the harvested power through Faraday's law. The stationary joint probability density function of the relative displacement and velocity is obtained in separable form by the solution of the corresponding FPK equation as in Daqaq [26]. The equivalent linearization technique is used to verify the statistics obtained from the FPK equation approach.

The present paper further investigates the problem of energy harvesting from the piezomagnetoelastic nonlinear oscillator of the cantilever beam considered by Litak et al. [18] and Ali et al. [20] subjected to Gaussian white noise excitation by solution of the corresponding FP equation. In this way the probability structure of the response and the generated voltage in the piezoelectric layers are directly obtained. The FP equation is derived for the electro-mechanical system consisting of

the coupled system of nonlinear equations representing the vibration of the cantilever beam in its first mode and the voltage generated in the piezoelectric patches. The energy harvesting mechanism in this case is very different from that considered by Daqaq [26] and Green et al. [27]. The energy harvesting mechanism is through the voltage generated from the piezoelectric patches attached to the root of the cantilever beam [18,20]. The electro-mechanical coupling arises from the mechanical force assumed proportional to the voltage across the piezo-electric material. The voltage across the load resistance arises from the mechanical strain through electro-mechanical coupling and the capacitance of the piezo-electric patches. This results in an additional first-order differential equation in terms of the time derivative of the voltage, voltage and velocity of the oscillator making the entire energy harvesting system a third-order coupled system. The corresponding FPK equation does not admit a closed form solution. The FE method developed in Pankaj and Narayanan [24] is used to solve the FP equation and the joint and marginal PDFs of the response of the beam and the voltage are obtained. The mean square values of these are also obtained from the corresponding PDFs.

The FE method is first applied to the solution of the FP equation of the energy harvesting problem of the nonlinear oscillator with an inductive power generator considered by Daqaq [26] for the two cases of white noise and coloured noise excitations. The FE results compare very well with Daqaq's results.

In the case of the piezomagnetoelastic energy harvester considered in this paper the results of the FE method compare very well with Monte Carlo simulation (MCS) results. The results show that higher intensities of the white noise excitation above a threshold result in better energy harvesting which is attributed to the jumps in the response from one potential well to the other. The effect of changing the system parameters on the mean square voltage is also investigated. It is observed that the electromechanical coupling coefficient has a significant effect on the mean square voltage, larger the coupling coefficient greater is the mean square voltage. The mean square voltage is observed to attain a maximum with respect to the cubic and linear stiffness parameters.

The paper is organized as follows. A brief introduction to the FP equation of nonlinear stochastic system and the magnetopiezoelastic nonlinear oscillator subjected to Gaussian white noise excitation is presented in Section 2 and the corresponding FP equation derived. The FE method of solving the FP equation is described in Section 3. A brief description of the MCS method adopted to verify the FE results is given in Section 4. The results of the solution of the FP equation by the FE method are presented and discussed in Section 5. Important conclusions of the paper are given in Section 6.

2. Fokker–Planck equation of nonlinear energy harvester

Consider the ferromagnetic cantilever beam [14] shown in Fig. 1 supported between two symmetric permanent magnets near the free end and subjected to support random Gaussian white noise excitation. Piezoelectric layers are bonded to the cantilever beam near the root and connected to an electrical load. The voltage generated from the piezoelectric layers across the load due to the random excitation contributes to the energy harvesting. The placement of the symmetric magnets is chosen so that the beam has two stable equilibrium positions and one unstable equilibrium position simulating the classical Duffing oscillator with double well potential.

The equations of motion of the beam corresponding to its first natural mode and the voltage generated in the piezoelectric layers can be expressed in nondimensional form by the following coupled nonlinear electro-mechanical equations [18]:

$$\ddot{X}+c\dot{X}+k(-X+\alpha X^3)-\chi V=\sigma W(t), \tag{1}$$

$$\dot{V}+\lambda V+\beta\dot{X}=0, \tag{2}$$

where X is the dimensionless transverse displacement of the beam tip, V is the dimensionless voltage across the load resistance, χ and β are the dimensionless piezoelectric coupling coefficients 'in the two equations, c is an assumed damping coefficient of the viscous type, $\lambda=1/R_lC_p$ is the reciprocal of the dimensionless time constant of the electrical circuit, R_l is the load resistance, C_p is the capacitance of the piezoelectric material, α is a nonnegative constant. $W(t)$ is a stationary, zero

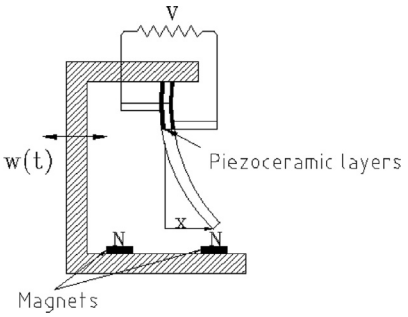

Fig. 1. Piezomagnetoelastic cantilever beam subjected to random excitation.

mean unit Gaussian white noise process with $E[W(t)W(t+\tau)]=\delta(\tau)$, σ is the intensity of excitation. The two sided power spectral density of the white noise excitation on the RHS of Eq. (1) corresponding to this intensity is $\sigma^2/2\pi$.

Eqs. (1) and (2) can be expressed in state space form by introducing the variables $X_1=X$, $X_2=\dot{X}$ and $X_3=V$, as

$$\begin{Bmatrix} \mathrm{d}X_1(t) \\ \mathrm{d}X_2(t) \\ \mathrm{d}X_3(t) \end{Bmatrix} = \begin{Bmatrix} X_2 \\ k(X_1-\alpha X_1^3)-cX_2+\chi X_3 \\ -\beta X_2-\lambda X_3 \end{Bmatrix} \mathrm{d}t + \begin{Bmatrix} 0 \\ \sigma \\ 0 \end{Bmatrix} \mathrm{d}B(t), \tag{3}$$

where $B(t)$ is the unit Wiener process.

The probabilistic response of multidimensional vibrational systems under Gaussian white noise random excitations in general can be considered to be governed by the following set of first-order stochastic differential equations (SDEs):

$$\dot{\mathbf{X}}(t)=\mathbf{m}[\mathbf{X},t]\,\mathrm{d}t+\mathbf{G}[\mathbf{X},t]\mathbf{W}(t), \tag{4}$$

where $\mathbf{X}(t)$ is the random response vector process, vector $\mathbf{m}[\mathbf{X},t]$ is related to the drift vector and matrix $\mathbf{G}[\mathbf{X},t]$ is related to the diffusion matrix and $\mathbf{W}(t)$ is the Gaussian white noise random vector process with appropriate dimensions [24]. The response $\mathbf{X}$ forms a Markov vector process whose transition PDF $p(\mathbf{X},t|\mathbf{X}^0,t_0)$ is governed by an appropriate Fokker–Planck (FP) equation. The FP equation associated with Eq. (4) can be derived from the Itô SDE of the form [28]:

$$\mathrm{d}\mathbf{X}(t)=\mathbf{m}[\mathbf{X},t]\,\mathrm{d}t+\mathbf{h}[\mathbf{X},t]\,\mathrm{d}\mathbf{B}, \tag{5}$$

where $B(t)$ is the normalized Wiener process [29] and the corresponding FP equation of $\mathbf{X}(t)$ is given by [30]

$$\frac{\partial p(\mathbf{X},t|\mathbf{X}^0,t_0)}{\partial t}=\left[-\sum_{i=1}^{N}\frac{\partial[m_i(\mathbf{X},t)]}{\partial X_i}+\frac{1}{2}\sum_{i=1}^{N}\sum_{j=1}^{N}\frac{\partial^2[h_{ij}(\mathbf{X},t)]}{\partial X_i\partial X_j}\right]p(\mathbf{X},t|\mathbf{X}^0,t_0), \tag{6}$$

where $p(\mathbf{X},t)$ is the joint PDF of the N-dimensional system state $\mathbf{X}$ at time t, m_i is the i-th element of the drift vector and h_{ij} is the ij-th element of the diffusion matrix $\mathbf{h}$. $m_i[\mathbf{X},t]$ may include Wong and Zakai correction terms if there is coupling between some of the response variables and excitation components as in the case of parametric excitation [29].

The transition PDF $p(\mathbf{X},t|\mathbf{X}^0,t_0)$ should satisfy the normalization condition, initial condition and the boundary conditions at infinity, given respectively by the following equations:

$$\int_{-\infty}^{\infty}p(\mathbf{X},t|\mathbf{X}^0,t_0)\,\mathrm{d}\mathbf{X}=1, \tag{7}$$

$$\lim_{t\to 0}p(\mathbf{X},t|\mathbf{X}^0,t_0)=\delta(\mathbf{X}-\mathbf{X}^0), \tag{8}$$

$$p(\mathbf{X},t|\mathbf{X}^0,t_0)|_{X_i\to\pm\infty}=0 \quad (i=1,\ldots,n). \tag{9}$$

The stationary solution of the FP equation is obtained by letting $\partial p(\mathbf{X},t|\mathbf{X}^0,t_0)/\partial t=0$.

Eqs. (3) of the energy harvesting system are of the form of the SDE (5) and the corresponding FP equation can be expressed as per Eq. (6) as

$$\frac{\partial p}{\partial t}=-X_2\frac{\partial p}{\partial X_1}+\left(cX_2-k\left(X_1-\alpha X_1^3\right)-\chi X_3\right)\frac{\partial p}{\partial X_2}+ (\beta X_2+\lambda X_3)\frac{\partial p}{\partial X_3}+\frac{\sigma^2}{2}\frac{\partial^2 p}{\partial X_2^2}+(c+\lambda)p \tag{10}$$

where $p=p(\mathbf{X},t|\mathbf{X}^0,t_0)$ the joint transition PDF of the state variables is used for notational convenience satisfying the conditions given by Eqs. (7)–(9).

In the next section the finite element (FE) method of solution of the FP equation is briefly presented.

3. Finite element method

The finite element equations are derived using the Galerkin projection of the FP equation. The solution domain, Ω, of the phase space consisting of the space variables is discretized into a collection of N_E elements, each element hosting n interpolating nodes and spanning the domain Ω_e. Let $\{\psi_1(\mathbf{X}),\ldots,\psi_n(\mathbf{X})\}$ represent a set of global cardinal interpolation functions defined on the solution domain. Using the Galerkin method, time varying solution $p(\mathbf{X},t)$ of the FP equation can be written as a linear combination in terms of the prior unknown values p_r of the probability densities at the global interpolation nodes, and the associated global cardinal basis functions $\{\psi_r(\mathbf{X})\}_{r=1}^{n}$ [24]

$$p(\mathbf{X},t)\approx\sum_{r=1}^{N_G}p_r(t)\psi_r(\mathbf{X}), \tag{11}$$

where N_G is the number of unique global nodes. Substitution of Eq. (11) into Eq. (10) leads to the following expression for the residual error:

$$\Re(\mathbf{X},t)=\sum_{r=1}^{N_G}\left[\frac{\partial p_r(t)\psi_r(\mathbf{X})}{\partial t}-\boldsymbol{L}_{FP}\left[p_r(t)\psi_r(\mathbf{X})\right]\right] \tag{12}$$

where $\boldsymbol{L}_{FP}[\cdot]$ is a partial differential FP operator corresponding to Eq. (6). Requiring the error term due to the FE approximation to be orthogonal to the basis functions, the equation error $\Re(\mathbf{X},t)$ is projected onto a set of independent weighting functions for the PDF. Taking the inner product of residual error on $L_2(\Omega)$, the space of Lebesgue integral functions, we get

$$\langle\Re(\mathbf{X},t),\psi_s(\mathbf{X})\rangle=0, \tag{13}$$

where $\langle\cdot\rangle$ is the L_2 inner product. The weight function $\{\psi_s(\mathbf{X})\}$ represents the space over which the projection of the equation error is minimized. Hence, Eq. (13) represents a finite set of differential equations in the following form:

$$\sum_{r=s}^{N_G}\dot{p}_t(t)\langle\psi_r(\mathbf{X}),\psi_s(\mathbf{X})\rangle-\sum_{r=s}^{N_G}p_r(t)\langle\boldsymbol{L}_{FP}\{\psi_r(\mathbf{X})\},\psi_s(\mathbf{X})\rangle=0. \tag{14}$$

Since the FP equation is of second order, it is required that the interpolation functions be twice differentiable. This requirement is weakened by using integration by parts and distributing the second derivative equally between the weight function and the interpolation function. Taking the inner product of the weighting function $\{\psi_i(\mathbf{X})\}$, with the FP equation and applying the divergence theorem, leads to the weak form of the FP equation

$$\mathbf{M}\dot{\mathbf{p}}+\mathbf{K}\mathbf{p}=\mathbf{0}, \tag{15}$$

subject to the initial condition $\mathbf{p}(0)=\mathbf{p}$, where, $\mathbf{p}$ is a vector of the joint PDF at the nodal points, where

$$\mathbf{M}=\{\langle\psi_r,\psi_s\rangle\}_{\Omega}, \tag{16}$$

$$\mathbf{K}=\int_{\Omega}\left[\sum_{i=1}^{N}\psi_r(\mathbf{X})\frac{\partial[m_i(\mathbf{X})\psi_s(\mathbf{X})]}{\partial X_i}\right]\mathrm{d}\mathbf{X}+\int_{\Omega}\left[\sum_{i=1}^{N}\sum_{j=1}^{N}\frac{\partial[\psi_r(\mathbf{X})]}{\partial X_i}\,\frac{\partial[h_{ij}\psi_s(\mathbf{X})]}{\partial X_j}\mathrm{d}\mathbf{X}\right]. \tag{17}$$

A solution of Eq. (15) is obtained using the Crank–Nicholson method, which is an implicit time integration scheme with second-order accuracy and unconditional stability and allows large time steps to be used. The time discretized equation takes the form:

$$[\mathbf{M}-\Delta t(1-\theta)\mathbf{K}]\mathbf{p}(t+\Delta t)=[\mathbf{M}+\Delta t\theta\mathbf{K}]\mathbf{p}(t), \tag{18}$$

where the parameter $\theta=0.5$ and Δt is the time step.

The three dimensional twenty noded isoparametric solid element as shown in Fig. 2 is chosen for the FE discretization. In terms of the normalized coordinates ξ,η,τ. The shape functions for the corner nodes are of the form:

$$\psi_i=\tfrac{1}{8}(1+\xi\xi_i)(1+\eta\eta_i)(\xi\xi_i+\eta\eta_i+\tau\tau_i-2), \tag{19}$$

while for a typical mid-side node with $\xi_i=0$, $\eta_i=\pm1$, $\tau_i=\pm1$ they are given by

$$\psi_i=\tfrac{1}{8}(1-\xi^2)(1+\eta\eta_i)(1+\tau\tau_i), \tag{20}$$

where ξ_i,η_i,τ_i are the normalized coordinates at node i. A reduced 14 points integration rule [31] is used for evaluating the stiffness like matrix $\mathbf{K}$ in Eq. (17) for the integration which gives a good accuracy with less computational effort of almost similar order as using $3\times3\times3$ integration scheme which involves greater computational effort. Of these 14 points, six correspond to three pairs of points situated symmetrically along each axis of symmetry and remaining eight correspond to

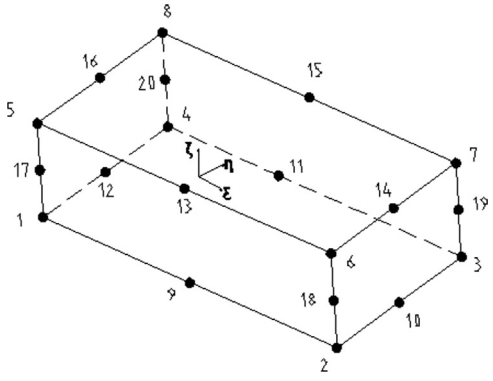

Fig. 2. Quadratic element with 20 nodes.

those situated symmetrically about each plane of symmetry just similar to $2\times2\times2$ Gauss rule in the case of 8 noded solid elements.

4. Monte Carlo simulation

In order to check the accuracy of the solution of the FP equation obtained by the FE method Monte Carlo Simulation (MCS) is used for the system of Eqs. (3). The MCS is a direct numerical method which involves the sampling of the underlying probability space to generate a family of sample functions of the excitation and generating a corresponding family of sample functions of the response by numerical integration of the nonlinear set of equations to each individual excitation from which the probability structure and statistics of the response can be obtained.

The idea of MCS is to generate samples of the random force compatible with its power spectral density and to solve Eq. (3) numerically for the response for every realization of the random force. For each given sample path (realization) of the Brownian motion, Eq. (3) becomes deterministic. Due to the unique differential rules (Itô formula) of stochastic integrals, the numerical schemes for discretizing Eq. (3) are quite different from the ones for smooth deterministic differential equations. The Euler–Maruyama (EM) discretization of Eq. (3) gives [32]

$$X_{n+1}^k = X_n^k + m(X_n^k, t_n)\Delta t + g(X_n^k, t_n)\Delta B_n^k \tag{21}$$

The noise increments ΔB_n^k are $N(0,\Delta t_n)$ distributed independent normal random variables which can be generated numerically by pseudo-random number generators. An efficient way to evaluate the increments of the Wiener process ΔB_n is to consider

$$\Delta B_n^k = B^k(t_{n+1}) - B^k(t_n) = \sqrt{t_{n+1}-t_n}N(0,1) \tag{22}$$

Discretized Brownian paths are generated to compute the increments $B^k(t_{n+1})-B^k(t_n)$ in Eq. (22) using Matlab function *randn* to generate unit normal variates which are scaled by the factor $\sqrt{t_{n+1}-t_n}$. For direct simulation of the Itô processes, it is important that the trajectories of the approximation be close to those of the Itô process and this leads to the concept of strong solution of the stochastic differential equation. The integration is performed using the forward EM numerical integration of Eq. (3), until the steady state is obtained for both the statistical properties and the PDF of the system response. On an average, the transition PDF is generated from a simulation of 2.5×10^5 realizations with a time step of 0.0005.

5. Results and discussion

5.1. FE method applied to the inductive type energy harvester

The finite element method presented in this paper is first applied to the energy harvesting problem considered by Daqaq [26] in which the following form of the Duffing oscillator is considered:

$$\ddot{X} - aX + bX^3 + c\dot{X} = \xi(t), \tag{23}$$

In Eq. (23) the damping coefficient c is an effective damping coefficient including electro-mechanical coupling effect of the inductive voltage generator and $\xi(t)$ is the Gaussian white noise with mean zero and $E(\xi(t)\xi(t_0)) = 2D\delta(t-t_0)$. The Fokker–Planck equation corresponding to Eq. (23) is

$$\frac{\partial p}{\partial t} = -X_2\frac{\partial p}{\partial X_1} + \frac{\partial(aX_1 - cX_2 - bX_1^3)p}{\partial X_2} + D\frac{\partial^2 p}{\partial X_2^2}. \tag{24}$$

For the stationary case, this admits a closed form solution for the joint PDF in separable form as [26]

$$p(X_1,X_2) = p(X_1)\times p(X_2) = A_1\exp\left(-\frac{c}{D}\left(-\frac{1}{2}aX_1^2 + \frac{1}{4}bX_2^4\right)\right)\times A_2\exp\left(-\frac{c}{2D}X_2^2\right) \tag{25}$$

where A_1 and A_2 are the normalization constants given by [26]

$$A_1^{-1} = \int_{\infty}^{\infty}\exp\left(-\frac{c}{D}\left(-\frac{1}{2}aX_1^2 + \frac{1}{4}bX_2^4\right)\right)dX_1, \quad A_2^{-1} = \int_{\infty}^{\infty}\exp\left(-\frac{c}{2D}X_2^2\right)dX_2 \tag{26}$$

These constants are derived as

$$A_1^{-1} = \left(\frac{2D}{bc}\right)^{0.25}\Gamma\left(\frac{1}{2}\right)\exp\left(\frac{a^2c}{8Db}\right)\Theta_{-0.5}\left(-\sqrt{\frac{a^2c}{2Db}}\right), \quad A_2^{-1} = \left(\frac{\pi D}{c}\right)^{0.5} \tag{27}$$

where $\Theta_{-0.5}$ is the Weber function. The joint PDF of displacement and velocity using the closed form solution of Eq. (25) and that obtained by the FE method for the parameters $c=0.05$, $D=0.05$, $a=1.5$ and $b=0.1$ are shown in Fig. 3. From the figure it is clear that they are in very good agreement. The contour plots of the joint PDFs by both the methods are shown in Fig. 4 again showing the close agreement between the two. In fact the results obtained by the FEM overlap on the results obtained by closed form solution. Marginal PDF of displacement for a specific velocity and marginal PDF of velocity for a specific

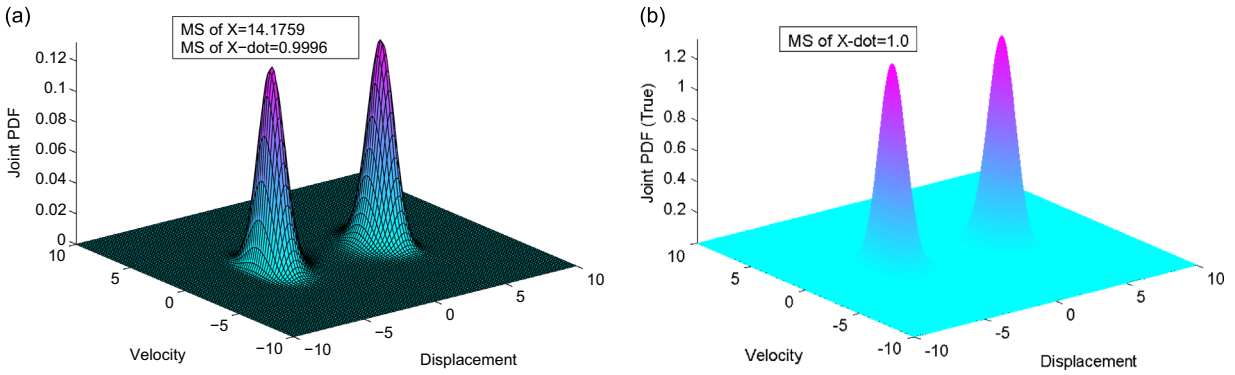

Fig. 3. Joint PDF of displacement and velocity of inductive energy generator (a) FEM and (b) Daqaq [26].

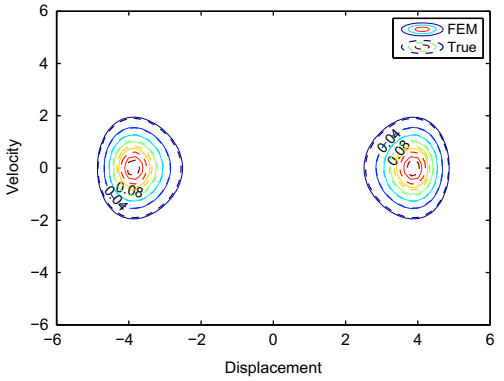

Fig. 4. Contour plot of joint PDF for inductive energy generator FEM and Daqaq [26].

displacement obtained by the closed form solution and the FE methods are shown in Fig. 5, once again showing the close agreement between the two.

The FE method is also applied to the other problem considered by Daqaq [26] in which the excitation $\xi(t)$ in Eq. (23) is of the Ornstein–Uhlenbeck process type having the exponential correlation function $E(\xi(t)\xi(t_0)) = 2D\gamma \exp^{-|t-t_0|}$.

$\xi(t)$ can be considered as the output of a linear first-order filter to white noise excitation given by

$$\dot{\xi} + \gamma\xi = \eta(t). \tag{28}$$

The corresponding joint PDF associated with Eqs. (23) and (28) is governed by the following FP equation:

$$\frac{\partial p}{\partial t} = -X_2 \frac{\partial p}{\partial X_1} + \frac{\partial (aX_1 - cX_2 - bX_1^3 + X_3)p}{\partial X_2} - \gamma \frac{\partial (X_3)p}{\partial X_3} + D\gamma \frac{\partial^2 p}{\partial X_2^2} \tag{29}$$

where $p(x, \dot{x}, \xi, t)$ is the joint PDF of $x, \dot{x}$ and ξ. Daqaq [26] obtained an approximate closed form solution for the joint PDF of x and $\dot{x}$, $p(x, \dot{x})$ for small noise intensity $\xi(t)$, neglecting the third variable ξ, by an iterative process of first obtaining the mean square value of displacement and using the same in the expression for mean square velocity and substituting in the separable form of the joint PDF. The FE method presented in this paper is also applied to this problem in which the joint PDF of $x, \dot{x}$ and ξ has been obtained. The mean square value of velocity for the parameters $c = D = 0.05$, $\gamma = 1$ for three different values of b, $b = 0.5$, 1 and 5 and the FE method are shown in Fig. 6. The mean square velocity obtained by the MCS method and by the approximate solution of Daqaq is also shown in the figure. It is observed that the results obtained by the FE method are closer to the MCS results than the approximate results of Daqaq.

5.2. FE method applied to the piezomagnetoelastic type energy harvester

In this section the FE method is applied to the problem under consideration in this paper namely the piezomagnetoelastic nonlinear energy harvester given by Eqs. (1) and (2). The FP equation corresponding to the piezomagnetoelastic nonlinear oscillator Eq. (10) is solved by the FE method. The following parameters are adopted for the oscillator $k = 0.5$, $\alpha = 1$, $\beta = 0.5$ and $\chi = 0.05$. The parameter λ is varied from 0.01 to 0.05 and the damping coefficient c is varied from 0.02 to 0.05. The intensity of the Gaussian white noise excitation is varied in the range 0.04–0.2. The space domain is chosen as $[-4, 4] \times [-4, 4] \times [-4, 4]$ which is discretized into a mesh of $50 \times 50 \times 50$ isoparametric elements. A typical solution run, required approximately 90 min on VEGA Super cluster having Dual Processor, Quad-core, Intel E5472 processor, at IIT Madras.

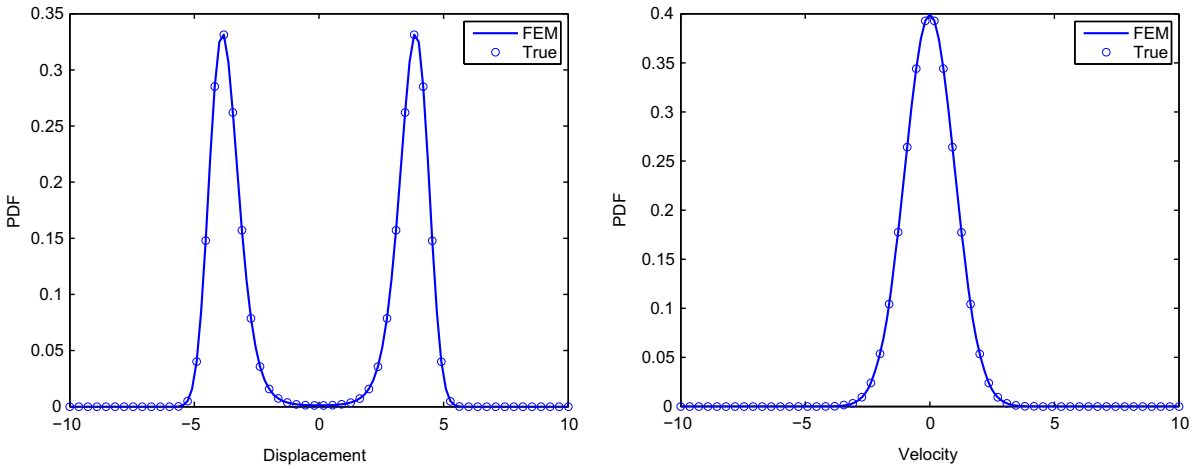

Fig. 5. Marginal PDF of displacement and velocity for inductive energy generator of Eq. (23), ____: FEM; ○: Daqaq [26].

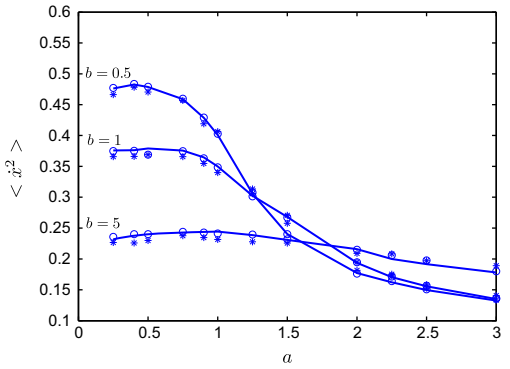

Fig. 6. Mean square velocity vs a: FP solution (____); MCS (○); approximate solution (Daqaq) (∗).

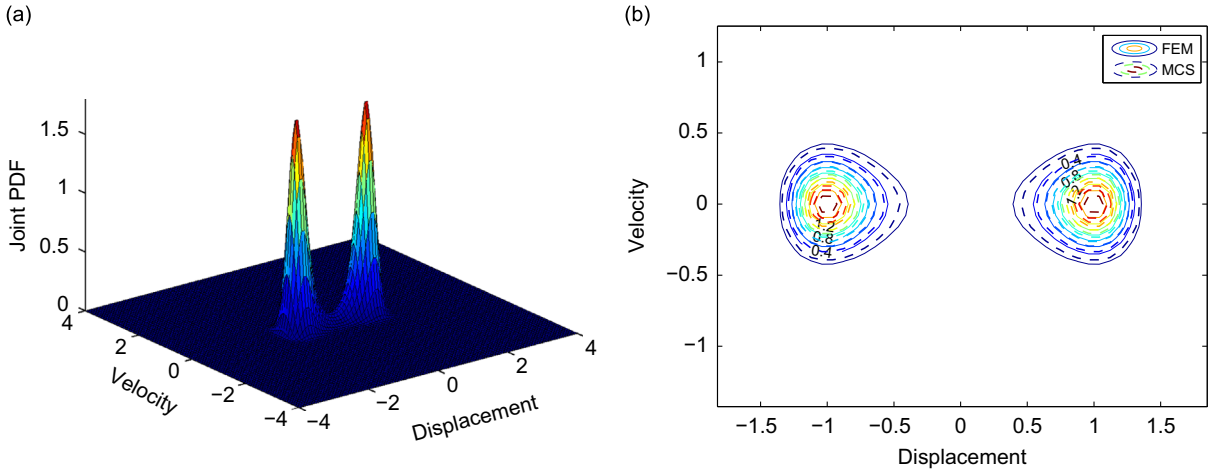

Fig. 7. (a) Joint PDF and (b) contour plot of piezomagnetoelastic energy harvester ($c=0.02$, $\lambda=0.01$, $\sigma=0.04$).

5.2.1. *Joint PDFs and marginal PDFs*

The joint PDF of the displacement and velocity for $c=0.02$, $\lambda=0.01$ and for different values of noise intensity σ ($\sigma=0.04, 0.1, 0.12$) and the corresponding contour plots are shown respectively in Figs. 7–9. At low levels of the noise intensity $\sigma=0.04$ the joint PDF shows sharp bimodal characteristics (Fig. 7) around the two equilibrium points of the deterministic nonlinear oscillator displaying some nonlinear interaction of the oscillator responding to the external random excitation. Looking at the corresponding contour plots of the joint PDFs it is observed that they resemble very much

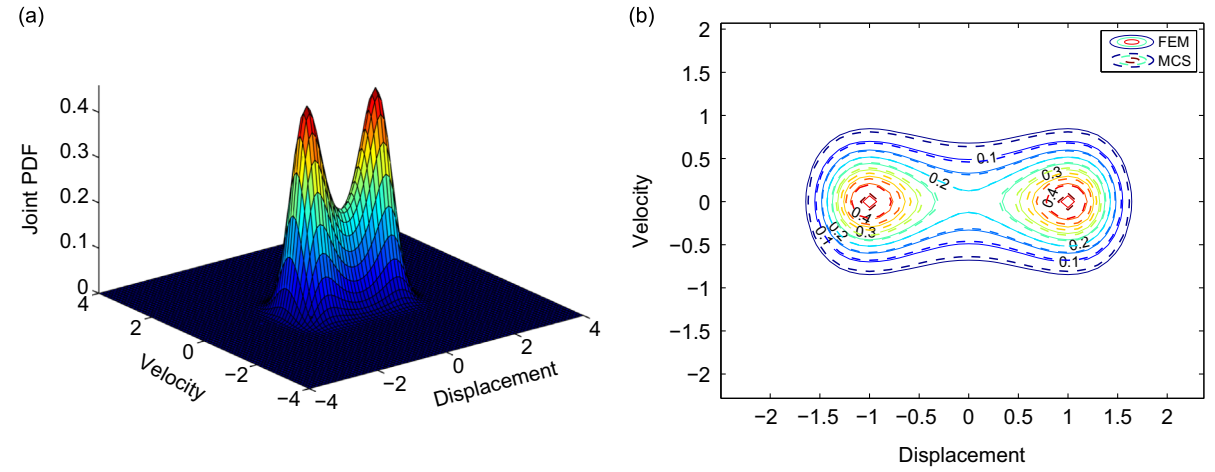

Fig. 8. (a) Joint PDF and (b) contour plot of piezomagnetoelastic energy harvester ($c=0.02$, $\lambda=0.01$, $\sigma=0.1$).

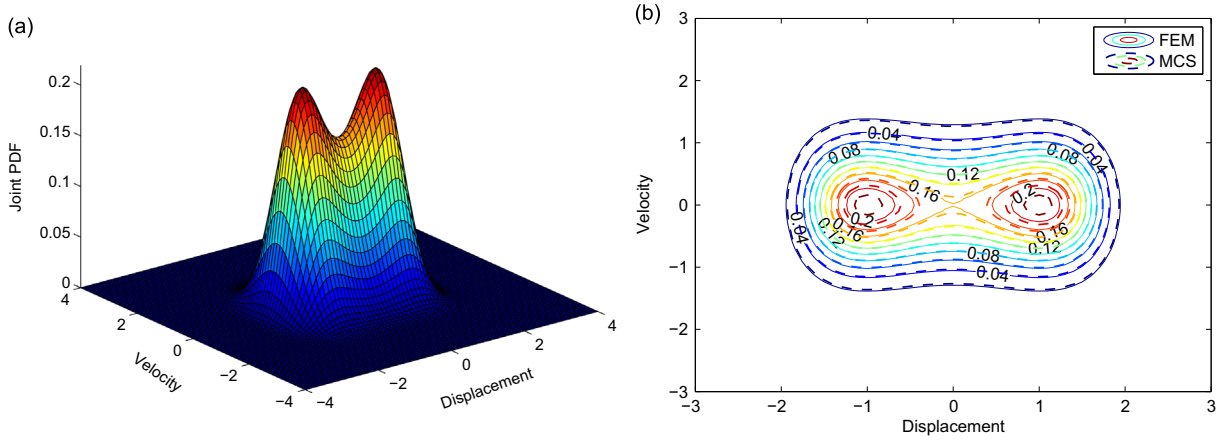

Fig. 9. (a) Joint PDF and (b) contour plot of piezomagnetoelastic energy harvester ($c=0.02$, $\lambda=0.01$, $\sigma=0.12$).

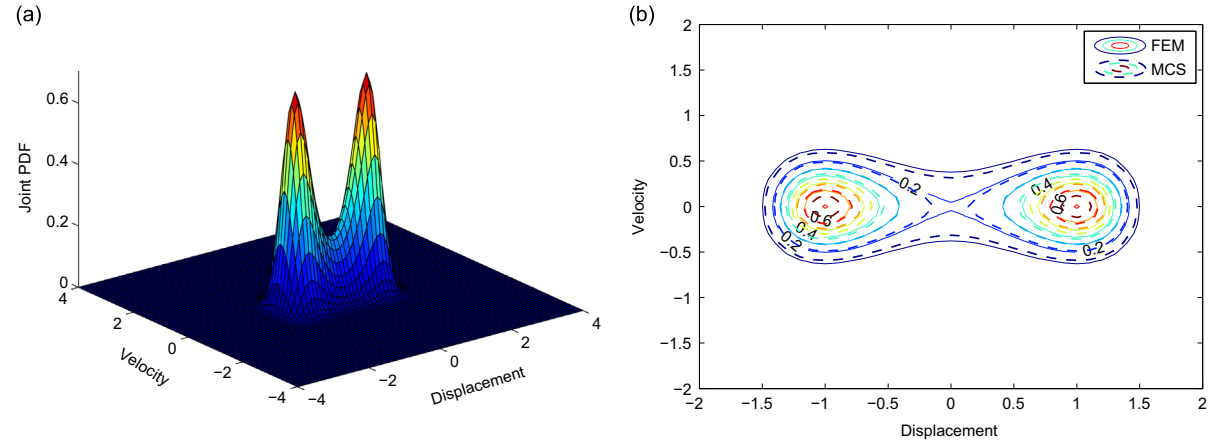

Fig. 10. (a) Joint PDF and (b) contour plot of piezomagnetoelastic energy harvester ($c=0.05$, $\lambda=0.01$, $\sigma=0.1$).

the phase portraits of the deterministic oscillator with the system states having a strong tendency (larger probability) of remaining near the two stable equilibrium points of the Duffing oscillator with the double well potential. The presence of the piezoelectric layer does not significantly alter the joint PDF of displacement and velocity. As the noise level is increased steeply to $\sigma=0.1$ and 0.12 (Figs. 8 and 9) the sharp bimodal peaks in the joint PDF tend to flatten and begin to merge

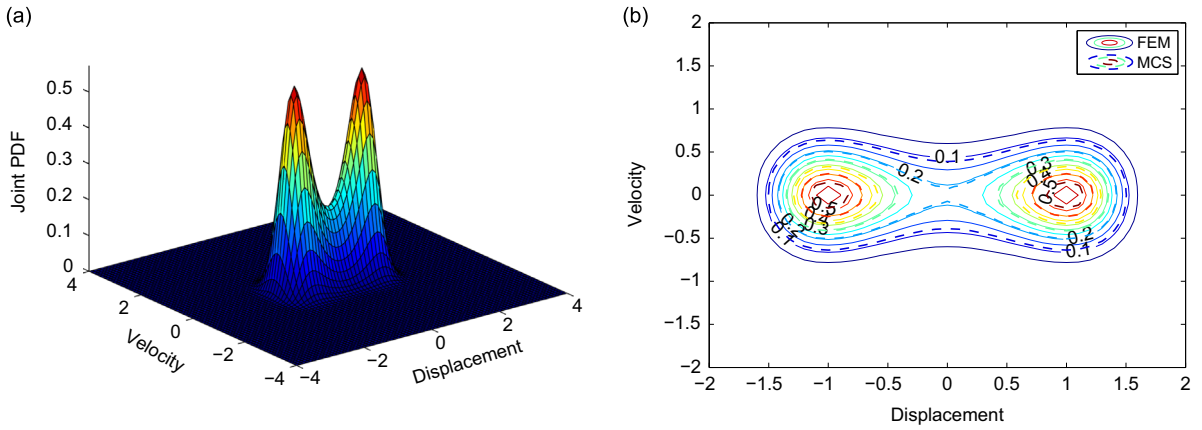

Fig. 11. (a) Joint PDF and (b) contour plot of piezomagnetoelastic energy harvester ($c=0.02$, $\lambda=0.05$, $\sigma=0.1$).

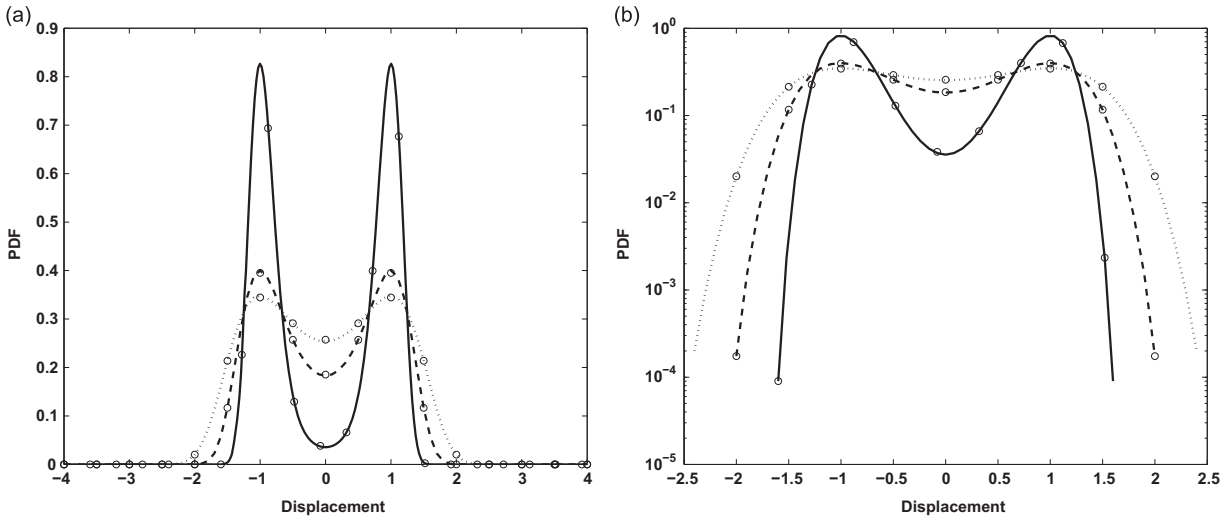

Fig. 12. Marginal PDF of displacement $c=0.02$, $\lambda=0.01$, (a) linear and (b) logarithmic plot; ($\sigma=0.04$ (____); $\sigma=0.1$ (- - - -); $\sigma=0.12$ (.....); MCS (○).

showing the enhanced nonlinear interactions and showing that the system response has a propensity to jump from one potential well to the other.

The joint PDF of the displacement and velocity and the corresponding contour plots for $\lambda=0.01$, $c=0.05$ and $\sigma=0.1$ are shown in Fig. 10 and for $\lambda=0.05$, $c=0.02$ and $\sigma=0.1$ are shown in Fig. 11. The marginal PDF of displacement, velocity and the voltage corresponding to Figs. 7–9 are shown in Figs. 12–14 respectively both in linear as well as in logarithmic plots. The MCS solutions are also shown in these figures by circles showing excellent agreement of the FP solution with the MCS results validating the FE method of solution of the FP equation. Logarithmic plots show that proposed FE solution gives impressively low order of error even at extremely small probability levels of the order of 10^{-4}. In Table 1, the values of the marginal PDF obtained by the FE method and the MCS results for $c=0.02$, $\lambda=0.01$ and $\sigma=0.1$ are given at a few grid points. It can be seen from the table that the values obtained by the FE method are accurate even at very low probability levels. Maximum absolute errors in the marginal density functions in the tail region are also given in the table.

The increase in noise intensity has the effect of enhancing the harvested energy as will be seen from the steep increase in the mean square voltage generated in the piezoelectric patches beyond a particular value of σ (Fig. 15). If the noise level is still further increased the two peaks tend to merge completely and the joint PDF diffuses around the phase space. The contour plots of the joint PDFs in these cases resemble the phase portraits of the Duffing oscillator corresponding to larger amplitudes of harmonic excitation the phase curves encircling both the equilibrium points. If the damping is increased to $c=0.05$ even for higher levels of noise intensity $\sigma=0.1$ the sharp bimodal nature of the joint PDF is maintained (Fig. 10). This shows that the larger the damping in the system the intensity of the noise has to be higher for a stronger interaction of the nonlinear system with the random excitation. Also for a given value of the damping $c=0.02$ if λ is increased to 0.05 the sharp bimodal character of the joint PDF of the response is preserved even for a larger intensity of noise $\sigma=0.1$ indicating that the time constant parameter of the electrical circuit has a similar influence as the damping coefficient c, in that larger the value of λ higher should be the noise intensity σ for a stronger nonlinear interaction. While the damping c directly influences the

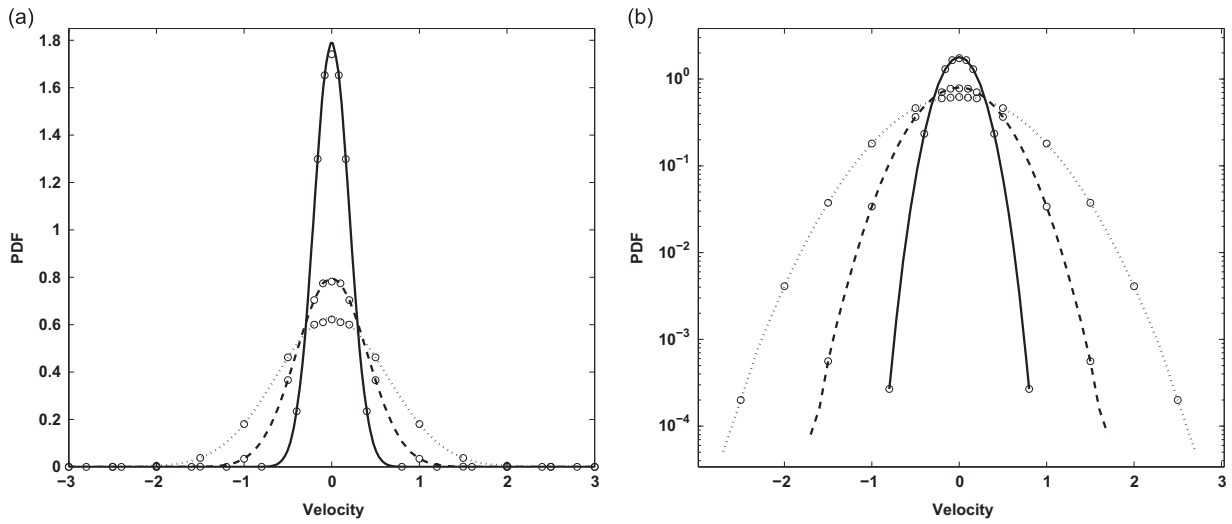

Fig. 13. Marginal PDF of velocity $c=0.02$, $\lambda=0.01$, (a) linear and (b) logarithmic plot; key as in Fig. 12.

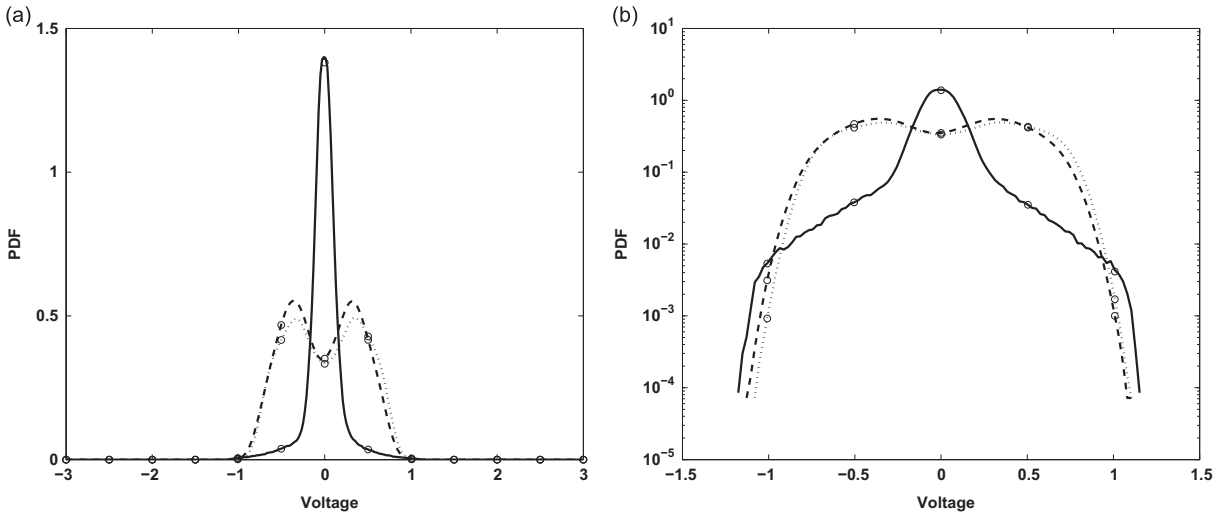

Fig. 14. Marginal PDF of voltage $c=0.02$, $\lambda=0.01$, (a) linear and (b) logarithmic plot; key as in Fig. 12.

dynamics of the structural oscillator, the time constant λ influences the dynamics of the nonlinear oscillator through the electromechanical coupling of the combined system. Similar observations as made from the joint PDF plots can also be made from the marginal PDF plots.

5.2.2. Mean square response and mean square voltage

The mean square values of the displacement, velocity and the voltage in the piezoelectric layers are calculated from the PDFs and are shown respectively in Fig. 15 as a function of white noise intensity for $c=0.02$ and 0.05 and for $\lambda=0.01$ and 0.05. It is seen from the figures that the mean square value of the displacement initially reduces with an increase in the excitation intensity, reaches a minimum value at a particular intensity, beyond which it increases with an increase in the excitation intensity. The mean square values of the velocity and voltage increase steadily with an increase in noise intensity. This is due to the bimodal nature of the marginal PDF of the displacement, with the displacement having higher probability to stay around the stable equilibrium points of the deterministic system for low levels of noise intensity. As the noise level increases as we have observed from the joint PDF and the marginal PDF the double peaks in the displacement PDF tend to merge signifying larger probability of the system response moving from one potential well to the other and vice versa. Up to around this threshold value of the noise intensity the mean square voltage is very small, beyond which the mean square voltage tends to steeply increase with the noise intensity and saturates at higher values of the noise intensity. Because of the increased values of mean square voltage there will be enhancement of the energy harvested. The value of the noise intensity at which the mean square voltage begins to increase rapidly can be adjusted by varying the parameters c and λ. Or for a given noise intensity the parameters c and λ can be suitably found to maximize the voltage mean square value in the

Table 1
Marginal PDF and maximum absolute error for energy harvesting in tail region.

Displacement	FEM	MCS	Velocity	FEM	MCS	Voltage	FEM	MCS
1.1	0.38715	0.38720805	1.1	0.01728	0.0173577	0.1	0.403908	0.4039636
1.2	0.344953	0.34499106	1.2	0.00816	0.0082477	0.2	0.48816	0.48823
1.3	0.276536	0.27662409	1.3	0.0036	0.00369	0.3	0.54846	0.54854506
1.4	0.194573	0.19467109	1.4	0.00152	0.0016197	0.4	0.5184006	0.518494
1.5	0.116692	0.11679187	1.5	0.00056	0.0006603	0.5	0.421968	0.422135
1.6	0.057825	0.0580055	1.6	0.00016	0.000467	0.6	0.30528	0.30567
1.7	0.022835	0.0236159	1.7	0.00008	0.000536	0.7	0.179488	0.180292
$\|p^{FEM} - p^{MCS}\|_\infty$	7.812×10^{-4}			4.56×10^{-4}			8.04×10^{-4}	

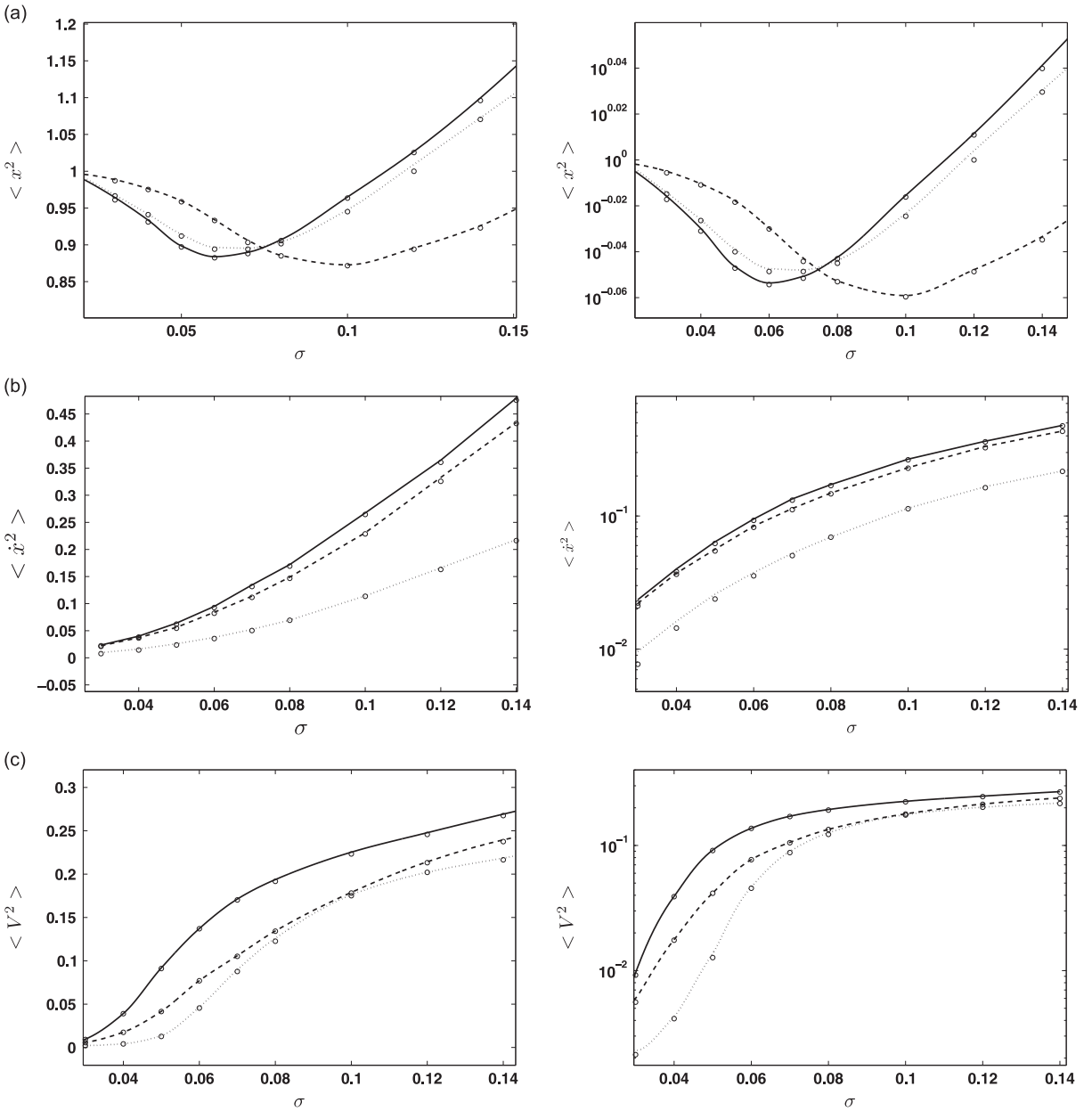

Fig. 15. Linear and logarithmic plot for mean square values: (a) displacement, (b) velocity, (c) voltage (____ (c=0.02, λ=0.01); - - - - (c=0.02, λ=0.05); ..... (c=0.05, λ=0.01); ○ (MCS).

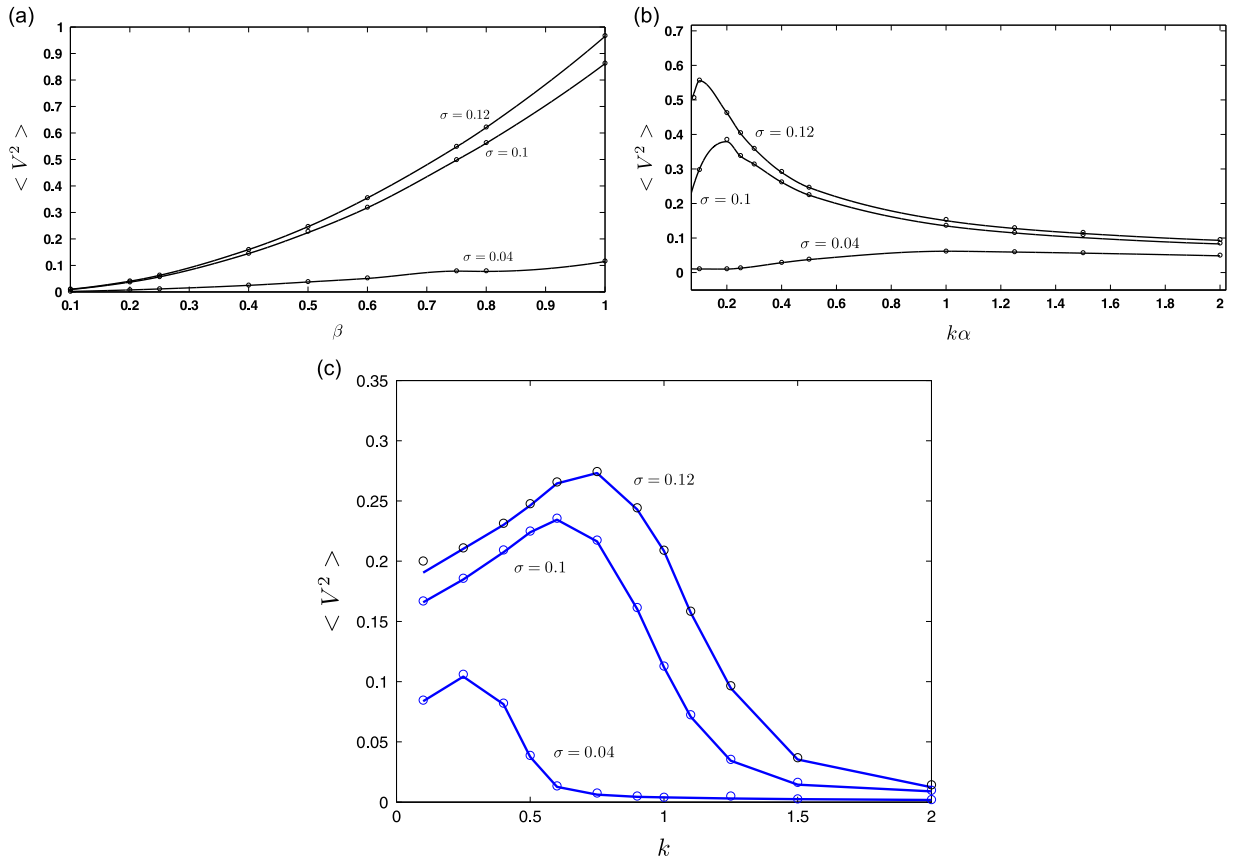

Fig. 16. Variation of the mean square voltage (a) with piezoelectric coupling coefficient β; (b) with nonlinear parameter $k\alpha$; (c) with linear parameter k for different value of noise intensity; FP solution (____); MCS (○).

piezoelectric layers. The mean square values obtained by MCS are also shown in the figures showing very good agreement between the two.

5.2.3. Effect of system parameters on the mean square voltage

In this section, the effect of the system parameters namely the electromechanical coupling coefficient β, the linear stiffness k, and cubic stiffness parameter $k\alpha$, on the mean square voltage for three different values of the noise intensity σ, σ=0.04, 0.1 and 0.12 are investigated. The other parameters adopted for the oscillator are χ=0.05, λ=0.01 and c=0.02.

In Fig. 16(a), the mean square voltage is plotted as a function of the electromechanical coupling coefficient β for k=0.5 and α=1. It is seen from the figure that the mean square voltage increases considerably with an increase in β. Thus the electromechanical coupling coefficient β has a significant effect on the energy harvesting capability.

Fig. 16(b) shows the variation of mean square voltage as a function of the nonlinear stiffness parameter $k\alpha$ for β=0.5 and k=0.5. It is observed that for a given value of noise intensity σ the mean square voltage increases with an increase in $k\alpha$, reaches a maximum and then decreases for a further increase in $k\alpha$.

Fig. 16(c) shows the variation of mean square voltage as a function of the linear stiffness parameter k for β=0.5 and $k\alpha$=0.5. In this case also for a given value of the noise intensity the mean square voltage attains a maximum value for a particular value of k.

The results shown in Fig. 16 indicate that the value of k corresponding to maximum mean square voltage increases with an increase in σ while the value of $k\alpha$ for maximum mean square voltage decreases with an increase in σ.

From the different patterns of variation of the mean square voltage with respect to the excitation noise intensity and the system parameters the possibility of enhancing the energy harvested from the nonlinear oscillator with optimum choice of the noise intensity and tuning of the system parameters can be further explored.

6. Conclusions

The Fokker–Planck equation corresponding to the nonlinear piezomagnetoelastic energy harvester excited by Gaussian white noise is derived. The finite element method is used to solve the Fokker–Planck equation for obtaining the joint and

marginal PDFs from which the statistics of the response of the oscillator and the mean square voltage are also obtained. The FE method is first applied to the two problems of the nonlinear inductive energy harvester considered by Daqaq [26] with close agreement between the two results. The results for the piezomagnetoelastic energy harvester obtained by the finite element method are validated by MCS. The effect of the intensity of the white noise excitation on the mean square voltage which is a measure of the energy harvested is investigated. As expected the mean square voltage increases with the excitation intensity. This increase becomes sharper beyond a threshold level of noise intensity which from the joint PDF plots of the response corresponds to the merging of the potential wells signifying higher probabilities of the response jumping from one potential well to the other. The effects of the system parameters on the mean square voltage are also studied. The mean square voltage increases with an increase in the electromechanical coupling coefficient while it has a maximum with respect to the linear stiffness parameter k and the nonlinear stiffness parameter $k\alpha$. The values of these parameters corresponding to the maximum vary with the noise intensity. Thus there is a good possibility of the choice of the noise intensity and the system parameters for effective energy harvesting.

Acknowledgements

The paper is a part of the work carried out under the Royal Society International Joint Project "Energy Harvesting from Randomly Excited Nonlinear Oscillators". The authors acknowledge the support of the Royal Society.

References

[1] H. Sodano, D. Inman, G. Park, A review of power harvesting from vibration using piezoelectric materials, *Shock and Vibration Digest* 36 (2004) 197–205.
[2] S.P. Beeby, M.J. Tudor, N.M. White, Energy harvesting vibration sources for microsystems applications, *Measurement Science and Technology* 17 (2006) 175–195.
[3] S.R. Anton, H.A. Sodano, A review of power harvesting using piezoelectric materials, *Smart Materials and Structures* 16 (2007) 1–22.
[4] S. Roundy, P.K. Wright, J. Rabaey, A study of low level vibrations as a power source for wireless sensor nodes, *Computer Communications* 26 (2003) 1131–1144.
[5] N.G. Stephen, On energy harvesting from ambient vibration, *Journal of Sound and Vibration* 293 (2006) 409–425.
[6] H. Sodano, D. Inman, G. Park, Generation and storage of electricity from power harvesting devices, *Journal of Intelligent Material Systems and Structures* 16 (2005) 67–75.
[7] S. Priya, Advances in energy harvesting using low profile piezoelectric transducers, *Journal of Electroceramics* 1 (2007) 165–167.
[8] F. Peano, Tambosso Design and optimization of a MEMS electret based capacitive energy scavenger, *Journal of Microelectromechanical Systems* 14 (2005) 429–435.
[9] J.M. Renno, M.F. Daqaq, D.J. Inman, On the optimal energy harvesting from a vibration source, *Journal of Sound and Vibration* 320 (2009) 386–405.
[10] E. Lefeuvre, A. Badel, C. Richard, D. Guyomar, Energy harvesting using piezoelectric materials: *case of random vibrations*, *Journal of Electroceramics* 19 (2000) 221–231.
[11] M.S.M. Soliman, E.M. Abdel-Rhhman, E.F. El-Saadany, R.R. Mansour, A wideband vibration based energy harvester, *Journal of Micromechanics and Microengineering* 18 (2008) 15021.
[12] E. Halvorsen, Energy harvesters driven by broadband random vibration, *Journal of Microelectromechanical Systems* 17 (2008) 1061–1071.
[13] S. Adhikari, M.I. Friswell, D.J. Inman, Piezoelectric energy harvesting from broad band random excitations, *Smart Materials and Structures* 18 (2009) 115005.
[14] A. Erturk, J. Hoffmann, D.J. Inman, A piezomagnetoelastic structure for broadband vibration energy harvesting, *Applied Physics Letters* 94 (2009) 254102.
[15] S.C. Stanton, C.C. McGehee, B.P. Mann, Reversible hysteresis for broadband magnetopiezoelastic energy harvesting, *Applied Physics Letters* 95 (2009) 174103.
[16] L. Gammaitoni, I. Neri, H. Vocca, Nonlinear oscillators for vibration energy harvesting, *Applied Physics Letters* 94 (2009) 164102.
[17] A.F. Arrieta, P. Hagedorn, A. Erturk, D.J. Inman, A piezoelectric bistable plate for nonlinear broadband energy harvesting, *Applied Physics Letters* 97 (2010) 104102.
[18] G. Litak, M.I. Friswell, S. Adhikari, Magnetopiezoelastic energy harvesting driven by random excitation, *Applied Physics Letters* 96 (2010) 214103.
[19] F.C. Moon, P.J. Holmes, A magnetoelastic strange attractor, *Journal of Sound and Vibration* 96 (1997) 275–296.
[20] S.F. Ali, S. Adhikari, M.I. Friswell, S. Narayanan, The analysis of piezomagnetoelastic energy harvesters under broadband random excitation, *Journal of Applied Physics* 109 (2011) 074904.
[21] A. Naess, V. Moe, Efficient path integration method for nonlinear dynamics system, *Probabilistic Engineering Mechanics* 15 (2000) 221–231.
[22] P. Kumar, S. Narayanan, Numerical solution of Fokker–Planck equation of nonlinear systems subjected to random and harmonic excitations, *Probabilistic Engineering Mechanics* 31 (2011) 455–473.
[23] B.F. Spencer Jr., L.A. Bergman, On the numerical solution of the Fokker-equations for nonlinear stochastic systems, *Nonlinear Dynamics* 4 (1993) 357–372.
[24] P. Kumar, S. Narayanan, Solution of Fokker–Planck equation by finite element and finite difference methods for nonlinear system, *Sadhana* 31 (4) (2006) 455–473.
[25] S.F. Wojtkiewicz, L.A. Bergman, B.F. Spencer Jr., High fidelity numerical solutions of the Fokker–Planck equation, in: ICOSSAR 97, The 7th International Conference on Structural Safety and Reliability, Kyoto, Japan 1997, 24–28.
[26] M.F. Daqaq, Transduction of a bistable inductive generator driven by white exponentially correlated Gaussian noise, *Journal of Sound and Vibration* 330 (2011) 2254–2664.
[27] P.L. Green, K. Worden, K. Atallah, N.D. Sims, The benefits of Duffing-type nonlinearities and electrical optimisation of a mono-stable energy harvester under white Gaussian excitations, *Journal of Sound and Vibration* 331 (2012) 4504–4517.
[28] T. Soong, M. Grigoriu, *Random Vibration of Mechanical and Structural Systems*, Prentice Hall, Englewood Cliffs, NY, 1993.
[29] E. Wong, M. Zakai, On the relation between ordinary and stochastic differential equation, *International Journal of Engineering Science* 3 (1965) 213–229.
[30] H. Risken, *The Fokker–Planck Equation*: *Methods of Solution and Applications*, Springer-Verlag, New York, 1989.
[31] T.K. Hellen, Effective quadrature rules for quadratic solid isoparametric finite element, *International Journal of Numerical Methods in Engineering* 4 (1972) 597–600.
[32] P.E. Kloeden, E. Platen, *Numerical solution of Stochastic Differential Equation*, Springer-Verlag, Berlin, 1992.